PALEOCEANOGRAPHY, VOL. 13, NO. 5, PAGES 491-501, OCTOBER 1998

Use of grain size and magnetic fabric analyses to distinguish among depositional environments

Leah H. Joseph, David K. Rea, and Ben A. van der Pluijm

Department of Geological Sciences, University of Michigan, Ann Arbor

Abstract. The combined use of grain size and magnetic fabric analyses provides the ability to discriminate among depositional environments in deep-sea terrigenous sediments. We analyzed samples from three different depositional settings: turbidites, pelagic or hemipelagic interlayers, and sediment drifts. Results indicate that sediment samples from these different environments can be distinguished from each other on the basis of their median grain size, sorting, as well as the intensity and shape of magnetic fabric as determined from an examination of the anisotropy of magnetic susceptibility. We use these discriminators to interpret downcore samples from the Bermuda Rise sediment drift. We find that the finer grains of the Bermuda Rise (relative to the Blake Outer Ridge) do not result from lower depositional energy (current speed) and so may reflect a difference in the nature of sediment being delivered to the site (i.e., distance from source) between the two locations.

1. Introduction

Paleoenvironmental interpretation of deep-sea terrigenous sediment depends on knowing the transport and depositional processes associated with each sedimentary horizon. The distinctions are sometimes obvious, but in many places, two or more sedimentary processes may alternate through time, such as eolian with hemipelagic processes, turbidites with pelagic or hemipelagic processes, and drift current with hemipelagic deposition. This variability of process at a single location is not always easily distinguished, and thus the true nature of the deposits and of the associated processes remains ambiguous [e.g., *Stow and Lovell*, 1979]. By using magnetic fabric analysis in conjunction with grain size data it is possible to determine which sedimentary process dominates at any given time. Grain size distributions permit reasonably good delineation among eolian, hemipelagic, ice-rafted, turbidity current, and drift deposits [e.g., *Rea and Hovan*, 1995; *Boven and Rea*, 1998]. Analysis of magnetic fabric permits differentiation between deposits resulting from random grain settling (pelagic or hemipelagic) and those resulting from ensuing transport along the seafloor (drifts and turbidites).

Ellwood and Ledbetter [1977, 1979], *Ellwood et al.* [1979], *Ledbetter and Ellwood* [1980], *Bulfinch et al.* [1982], and others introduced the combined use of magnetic fabric and grain size analyses approximately two decades ago in an effort to delineate past changes in current velocity. Our study examines the grain size distribution and magnetic fabric of sediment from three different depositional environments: turbidites, their pelagic or hemipelagic interlayers, and sediment drifts. It represents a test of methodology in depositional environment recognition where one would expect that variations in grain size and magnetic fabric would be most apparent. As a trial application of our methodology, we examine a second sediment drift core and interpret its depositional environment on the basis of our initial findings.

Paper number 98PA01939.
0883-8305/98/98PA-01939$12.00

2. Sampling and Methods

2.1. Cores and Samples

For this study, samples representing well-understood depositional settings were taken by one of the authors (DKR) from two cores raised by the R/V *Wecoma* and curated at Oregon State University and one core raised by the R/V *Cape Hatteras* and curated at the University of Minnesota, Duluth. The *Wecoma* cores (W8209-19GC and W8209-20GC) were raised from the distal portion of the Delgada deep-sea fan off northern California (Figure 1) and contain obvious thin turbidite sand and silt layers interspersed with finer-grained hemipelagic interlayers. These cores and others from this general region form the basis of studies by *Rea et al.* [1985] and *Karlin et al.* [1992]. The *Cape Hatteras* core (CH89-1P) is one of a series of cores raised from the crest of the Blake Outer Ridge (Figure 2) specifically as part of a project to understand the processes and history of drift current deposition and is a uniform gray silt. Selecting a core from the ridge crest decreases the possibility of sampling a turbidite deposit, and no turbidites were described in or observed during the sampling of CH89-1P. Nevertheless, localized downslope transport is still possible, and seismic records from the flanks of the Blake Outer Ridge do indicate the presence of blocky debris flows there [*Johnson et al.*, 1988; *Haskell*, 1991; *Haskell and Johnson*, 1993]. CH89-1P and the nearby cores form the basis for studies reported by *Johnson et al.* [1988], *Haskell* [1991], *Haskell et al.* [1991], *Haskell and Johnson* [1993], and *Schwartz et al.* [1997]. See Table 1 for core location information.

Samples from the third region studied, the Bermuda Rise (Figure 2), are from core CH89-9P and were provided along with core description notes by S.P. Lund (Table 1) [University of Southern California, written communication, 1996]. Those studying CH89-9P and nearby cores from the Bermuda Rise report these sediments to represent a drift deposit [*Laine and Hollister*, 1981; *Keigwin et al.*, 1984; *Keigwin and Jones*, 1989, 1994; *Lund and Keigwin*, 1994].

A 2.1 x 2.1 x 1.5 (or 2.0 x 1.9 x 1.5) cm plastic cube with sediment and a corresponding standard scoop sample were

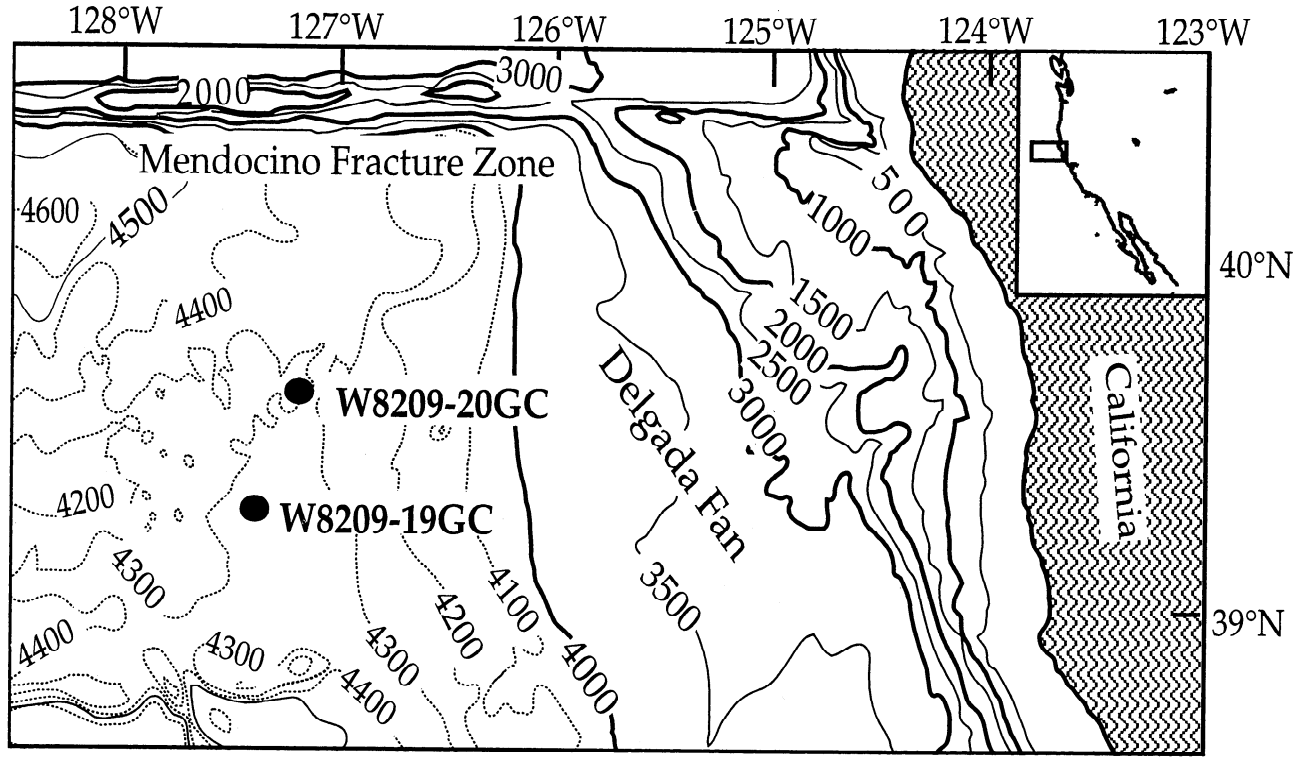

Figure 1. Location of cores containing both turbidites and their interlayers. Contours are given in meters. (Adapted from *Rea et al.* [1985], with permission from Elsevier Science.)

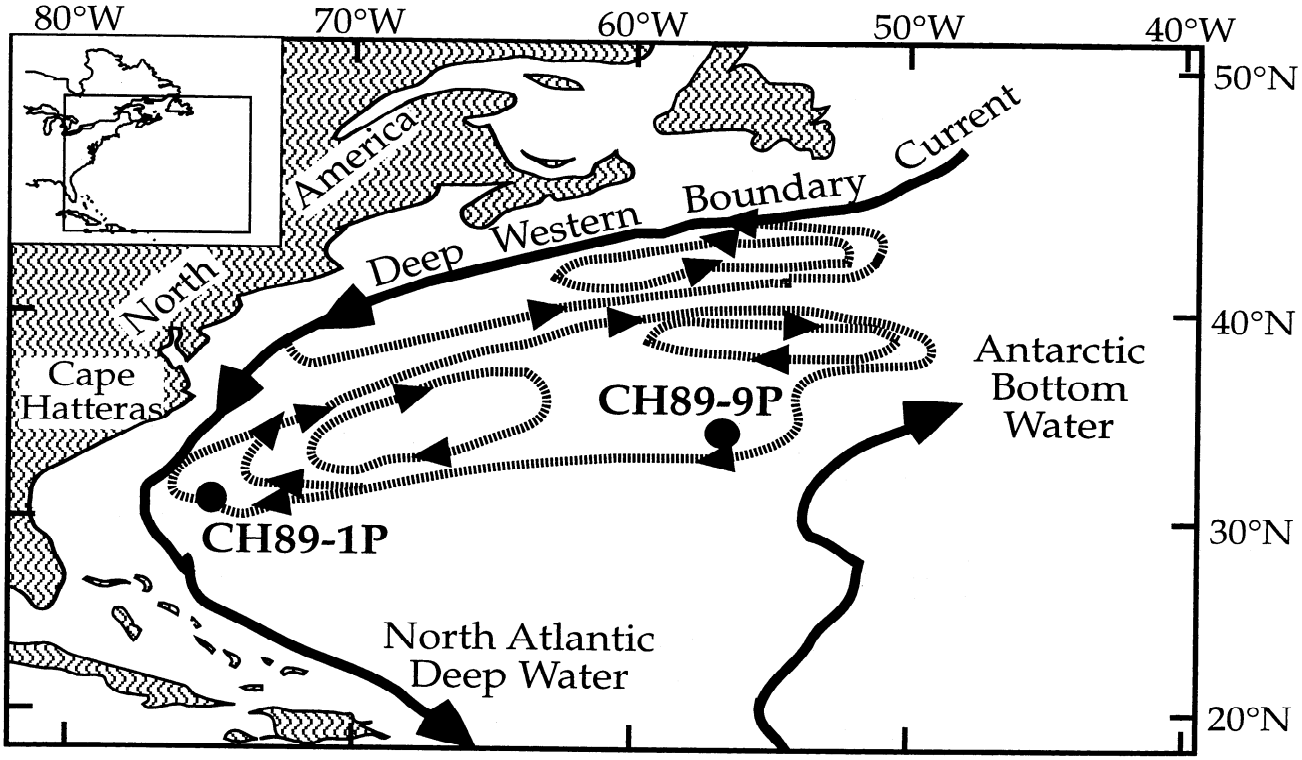

Figure 2. Location of Blake Outer Ridge and Bermuda Rise sediment drift cores. The dark solid lines represent the main deep water currents in the area, while the dashed lines show the direction of the deep recirculating gyres. (Adapted from *Keigwin and Jones* [1994].)

Table 1. Core Location Information

Core	Region	Latitude. N	Longitude. W	Depth (m)	Environment
W8209-19GC	Delgada Fan	39°16.4'	127°22.8'	4355	turbidites and
-20GC		39°35.7'	127°11.3'	4294	interlayers
CH89-1P	Blake Outer Ridge	31°15.0'	74°50.0'	3180	drift deposit
CH89-9P (near KNR31 GPC-5)	Bermuda Rise	(33°41.4)	(57°37.2')	(4583)	drift deposit

obtained from various depths in the W8209 and CH89-1P cores. The cubes were used for magnetic analyses. Homogenous mixtures of each of the scoop samples were used for extraction of terrigenous sediment and ensuing grain size analysis. For the Bermuda Rise core, corresponding scoop samples were not available, and the sediment in each cube was homogenized for grain size analyses when all magnetic work was completed.

2.2. Magnetic Analysis

2.2.1. Magnetic susceptibility. Anisotropy of magnetic susceptibility (AMS) analyses were done at the University of Michigan on a KLY-2 KappaBridge. Results of AMS analyses show the bulk orientation of grains in a sample, the magnetic fabric, and are represented in three-dimensional space by an ellipsoid; in most cases the greatest induced magnetization parallels the long axis whereas the weakest induced magnetization parallels the short axis [*Nye*, 1957, 1985; *Tarling and Hrouda*, 1993, and references therein]. This susceptibility ellipsoid represents the combined results of the susceptibility anisotropy produced by individual grain shape and/or crystallography in a sample, as well as the alignment of these grains within the sample.

The susceptibility ellipsoid is described here by two parameters: a corrected anisotropy degree (P') and a shape parameter (T) [*Jelinek*, 1981]. P', the magnitude of the anisotropy is:

$$P' = \exp\{2[(\eta_1 - \eta_m)^2 + (\eta_2 - \eta_m)^2 + (\eta_3 - \eta_m)^2]\}^{1/2}$$

where $\eta_1 = \ln \boldsymbol{k}_1$, $\eta_2 = \ln \boldsymbol{k}_2$, $\eta_3 = \ln \boldsymbol{k}_3$, $\eta_m = (\eta_1\ \eta_2\ \eta_3)^{1/3}$, and $\boldsymbol{k}_1 \geq \boldsymbol{k}_2 \geq \boldsymbol{k}_3$ are the principal susceptibilities (SI units). Higher values of P' represent stronger degrees of magnetic anisotropy. The maximum P' obtainable for a sample depends upon the dominant carrier of the anisotropy. In this study, five analyses on a single sample result in an average P' with a variability almost always < 0.01.

T defines the shape of the ellipsoid and is defined as

$$T = (2\eta_2 - \eta_1 - \eta_3)/(\eta_1 - \eta_3).$$

If $0 < T \leq 1$, then the ellipsoid is oblate (two long axes and one short axis; disk-shaped); if $-1 \leq T < 0$, then the ellipsoid is prolate (two short axes and one long axis; cigar-shaped); and if $T = 0$, then the ellipsoid is neutral (between oblate and prolate) or spherical if P' is near 1.0.

The orientation of the susceptibility ellipsoid can also be obtained so that the current direction of these primarily flat-lying sediments may be obtained. In fact, *Stow* [1979], *Ledbetter and Ellwood* [1980], and *Shor et al.* [1984] used the sediment fabric alignment direction to try to distinguish between interlayered sediment drift (along slope) and turbidite (down slope) deposits. However, these three studies are not in agreement regarding the ability to differentiate between turbidite and sediment drift deposits using the fabric orientation. This method is further complicated by the fact that the coring device commonly rotates as it penetrates the sediment. It is possible to realign the cores using other magnetic parameters. However, in this study of technique we focus primarily on methods of determining relative current intensity, rather than direction; the latter represents a planned addition to future studies.

2.2.2. Low-temperature experiments. Four to five samples from each of three different depositional environments and six samples from the Bermuda Rise core were subjected to low-temperature susceptibility experiments, as described by *Richter and van der Pluijm* [1994], to determine the mineralogy that dominates the magnetic susceptibility signal (i.e., paramagnetic or ferrimagnetic). The bulk magnetic susceptibilities were measured at room temperature and at ~77 K. If the magnetic susceptibility signal is controlled by paramagnetic or superparamagnetic (SP) minerals (i.e. clay minerals or very fine grained [<0.03 μm] magnetite), the bulk magnetic susceptibility of the sample should increase at low temperatures. No change in the bulk magnetic susceptibility would indicate that ferrimagnetic grains (i.e., magnetite) dominate the magnetic susceptibility signal.

To distinguish between SP and paramagnetic grains, we exposed representative samples at 77 K to a 1 Tesla magnetic field and then measured the magnetic intensity of the sample for ~45 min using a 2G Enterprises cryogenic magnetometer. SP grains will retain a magnetization while at 77 K, but the intensity will decay as the sample gets warmer; this exhibits itself as a decrease in the magnitude of the intensity of the field with time. In contrast, this magnitude should remain the same with time for ferrimagnetic or paramagnetic grains [*Freeman*, 1983].

2.2.3. Magnetic grain size experiments. We determined the magnetic grain size so that it could be compared to that of the overall grain size. As well, the magnetic grain size is used to evaluate the potential contribution of bacterial magnetite. Nine samples from the first part of this study (mostly turbidites and interlayers) were imparted with a partial anhysteretic remanence magnetization (pARM) using a Sapphire Instruments SI-4 AF demagnetizer, and then measured in the cryogenic magnetometer following the procedure given by *Jackson et al.* [1988]. Our primary interest lies in magnetic saturation curves that indicate the type of magnetic minerals in the sample by the strength of

field needed to saturate the sample and pARM peak positions that indicate the magnetic grain size. As an additional (relative) grain size indicator, we also imparted and measured the ARM of several samples and compared this to the bulk magnetic susceptibility. ARM is sensitive to smaller magnetic grains (single-domain through smaller pseudo-single-domain) whereas bulk susceptibility is more sensitive to coarser magnetic grains (pseudo-single-domain through multidomain). By comparing these two magnetic parameters the relative grain sizes may be obtained; in general, the ratio of ARM to the bulk susceptibility decreases with increasing grain size [*Banerjee et al.*, 1981].

2.3. Grain Size Analysis

2.3.1. Extraction process. The samples for size analysis were first freeze dried and then the terrigenous grains were extracted chemically. The chemical extraction process is based on a procedure described by *Rea and Janecek* [1981], with modifications by *Clemens and Prell* [1990] and *Hovan* [1995]. This process removes calcium carbonate, oxides and hydroxides, zeolites, and biogenic silica and isolates the terrigenous component of marine sediment. Once the chemical extraction process was completed, the resulting samples were placed in distilled deionized water with a dispersing agent to prevent grain flocculation.

2.3.2. Grain size analysis. Grain size analysis was performed using a Coulter Counter which draws grains, suspended in an electrolyte, through a small hole and electronically determines (for each sample) a measure of the volume of each grain passing through the aperture. For this project we used a 100 μm aperture which allows recognition and counting of all grains between 2 and 60 microns in diameter. The results are distributed into 256 size channels, or size divisions, between preset end values. By assuming that the grains are spheres equivalent to the true grain volume and are of equal density, grain diameters are converted to grain mass in order to obtain weight percent data. Samples were analyzed at least three times, with counts of 150,000 grains each.

The resulting grain size distribution plots are histograms of grain diameters versus weight percent where each point on the plot represents one of the 256 channels. This curve is described here by the median grain size (Φ_{50}, where $\Phi = -\log_2$(grain diameter in mm)) and the inclusive graphic standard deviation (IGSD = $[\{\Phi_{84} - \Phi_{16}\}/4] + [\{\Phi_{95} - \Phi_5\}/6.5]$). A larger IGSD implies poorer sorting, and the grain size distribution of a sample having a large IGSD will exhibit a broad curve rather than a distinct peak [*Folk*, 1974]. Results are given in both Φ units and microns and generally have a variability < ±0.05Φ for triplicate analyses.

3. Results

3.1. Grain Size and Magnetic Fabric Analyses

Almost all of the sediment samples fall into three distinct groups; each population corresponds to a different sedimentary environment (Figures 3 and 4; Tables A1 and A2[1] give grain size and magnetic information for all samples).

[1]Tables A1 and A2 are available electronically at World Data Center A for Paleoclimatology, NOAA/NGDC, Boulder, Colo. (e-mail: paleo@mail.ngdc.noaa.gov; URL: http://www.ngdc.noaa.gov./paleo).

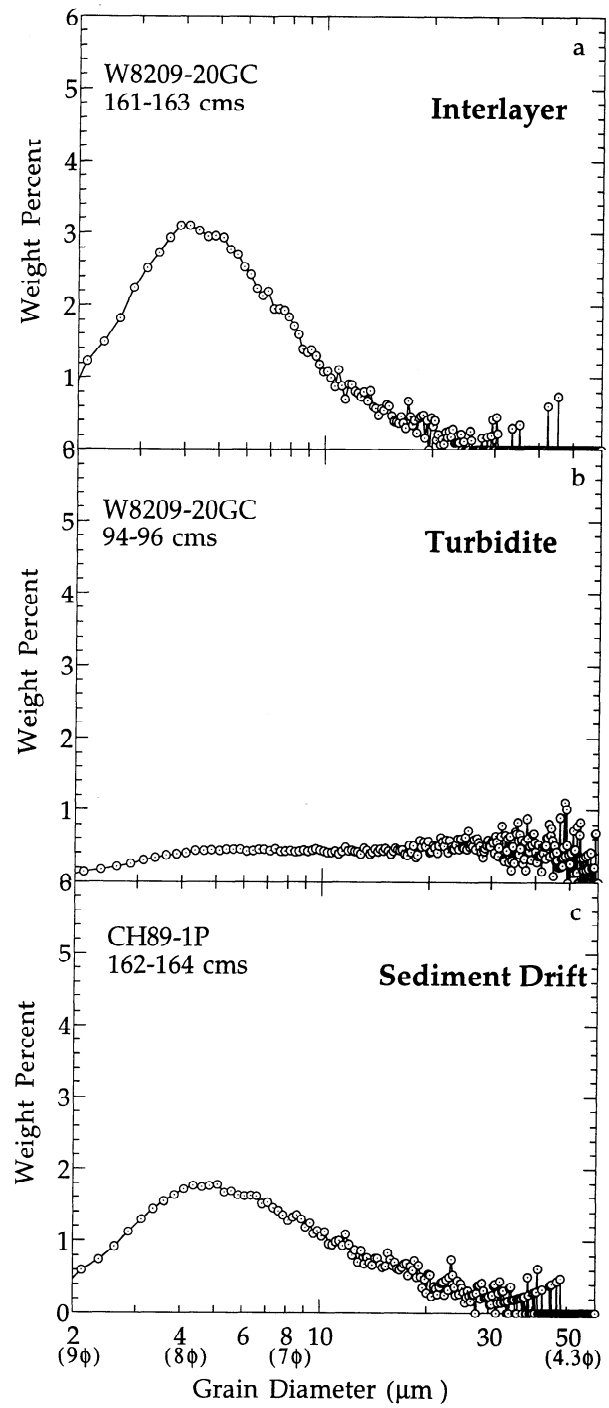

Figure 3. *Grain size distributions.* Characteristic grain size distributions of (a) an interlayer, (b) a turbidite, and (c) a sediment drift. Note the discrete distribution for each environment.

3.1.1. Interlayers (W8209-19GC, -20GC). The samples in this trend have a median grain size ranging from ~7.25 to 7.00Φ (6.7 to 7.8 μm). The IGSD ranges between ~0.89 and 1.01Φ; the samples exhibit moderate sorting [Folk, 1974] with a distinct peak in the grain size distribution at ~8Φ (4 μm; Figures 3a and 4a). The magnetic fabric of the interlayer samples is nonexistent to very weak; P' never exceeds 1.01, the equivalent fabric

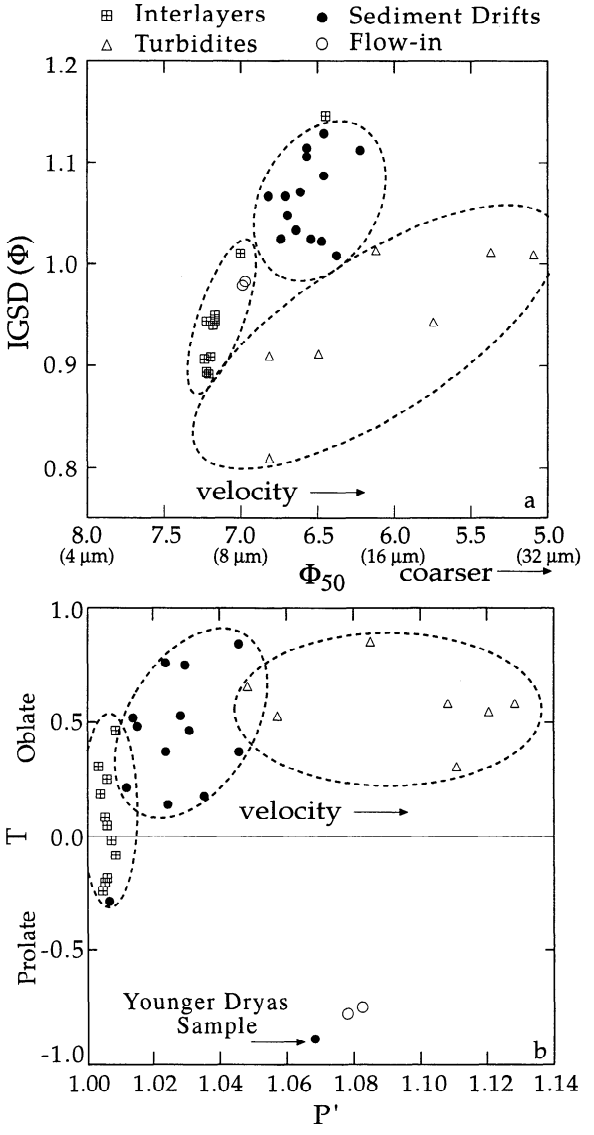

Figure 4. Grain size and magnetic fabric results for the three depositional environments: (a) median grain size (Φ_{50}) versus inclusive graphic standard deviation (IGSD) and (b) the strength of the anisotropy (P') versus the shape of the anisotropy (T). The dashed lines encircle the samples within a depositional environment and effectively represent their trends. Note how samples cluster into groups representing their depositional environment and the relationship of these factors with interpreted velocity of the current.

"shape" of these randomly oriented grains is a sphere (Figure 4b).

3.1.2. Turbidites (W8209-19GC, -20GC). This suite of samples has a broad grain size distribution with significant amounts of coarse, silt-sized material (0.81Φ < IGSD < 1.01Φ). Φ_{50} varies between ~6.80 and 5.08Φ (9.0 and 29.6 μm; Figures 3b and 4a). A well-developed magnetic fabric is present (P' > 1.05) and the susceptibility ellipsoid has typically oblate shapes (Figure 4b).

3.1.3. Sediment drift (CH89-1P). The sediment samples in this group have median grain sizes that vary between ~6.81 and 6.21Φ (8.9 and 13.5 μm) and exhibit fairly broad grain size distributions with only minor amounts of coarse silt-sized material (0.98Φ < IGSD < 1.13Φ; Figures 3c and 4a). The magnetic fabrics range between those of the interlayers and the turbidites; the magnetic fabric parameter P' generally ranges from 1.01 to 1.05, and ellipsoid shapes are primarily oblate ($0.1 < T < 0.9$; Figure 4b).

3.2. Low-Temperature Experiments

The ratios of bulk susceptibility at 77 K to bulk susceptibility at room temperature for interlayer samples range from 1.5 to 1.8 (Table A1). This is similar to the sediment drift samples, whose bulk susceptibility ratios range from 1.6 to 2.0. The bulk susceptibility ratios of the turbidites vary from 0.9 to 1.4. These low-temperature susceptibility experiments show that both (super) paramagnetic and ferrimagnetic grains contribute to the AMS signal, except for the coarsest of turbidites where the relationship between the AMS and the sample is controlled by the shape of the ferrimagnetic grains. This joint contribution is supported by low bulk susceptibilities, indicating that ferrimagnetic grains are not the dominant phase; however, the presence of ferrimagnetic grains is indicated by the ARM and pARM experiments, which respond only to ferromagnetic grains.

In our second low-temperature experiment, evidence of superparamagnetism would be seen as a decrease in the magnitude of the intensity of the induced magnetization with time. This was not observed in any of our samples, thus indicating that paramagnetic and not SP grains are contributing to the AMS signal.

3.3. Magnetic Grain Size

Magnetic saturation of the magnetic minerals in all samples examined occurred at ~100 mT as indicated by the leveling off of the normalized ARM curve (Figure 5). Therefore the magnetic grains in the sample are multidomain magnetites, rather than single-domain magnetites. Note that single-domain magnetites smaller than ~30 nm may behave superparamagnetically [*Dunlop,* 1990; *Tarling and Hrouda,* 1993], which provides additional evidence that SP grains do not contribute significantly to the AMS measurements.

The location of the pARM peak (in mT) gives the ferrimagnetic (not the overall) grain size [*Jackson et al.*, 1988]. As exemplified in Figure 5, the peaks of the normalized pARM curve for the interlayer, turbidite, and sediment drift samples all lie at ~30 mT, although there is a very slight difference in the magnetic grain size of these different environments (sediment drifts have the finest grains, while the turbidites have the coarsest grains). This result provides a ferrimagnetic grain size of ~2 μm (9Φ) for all three depositional environments.

The ratio of ARM to the bulk susceptibility provides information about relative grain size; in general, the larger the ratio, the smaller the magnetic minerals [*Banerjee et al.*, 1981; *King et al.*, 1982,]. The ratios of our samples also plot in groups according to their depositional environment and are ~14, 7, and 4 for drifts, interlayers, and turbidites, respectively (Figure 6). Since the ARM is more sensitive to finer grains this indicates not only that these grains are fine but that there is a variation in the magnetic grain size between these various environments. This analysis thus provides a more pronounced verification of the grain size trends observed by pARM. However, this method is a measure of relative grain size, and therefore the absolute

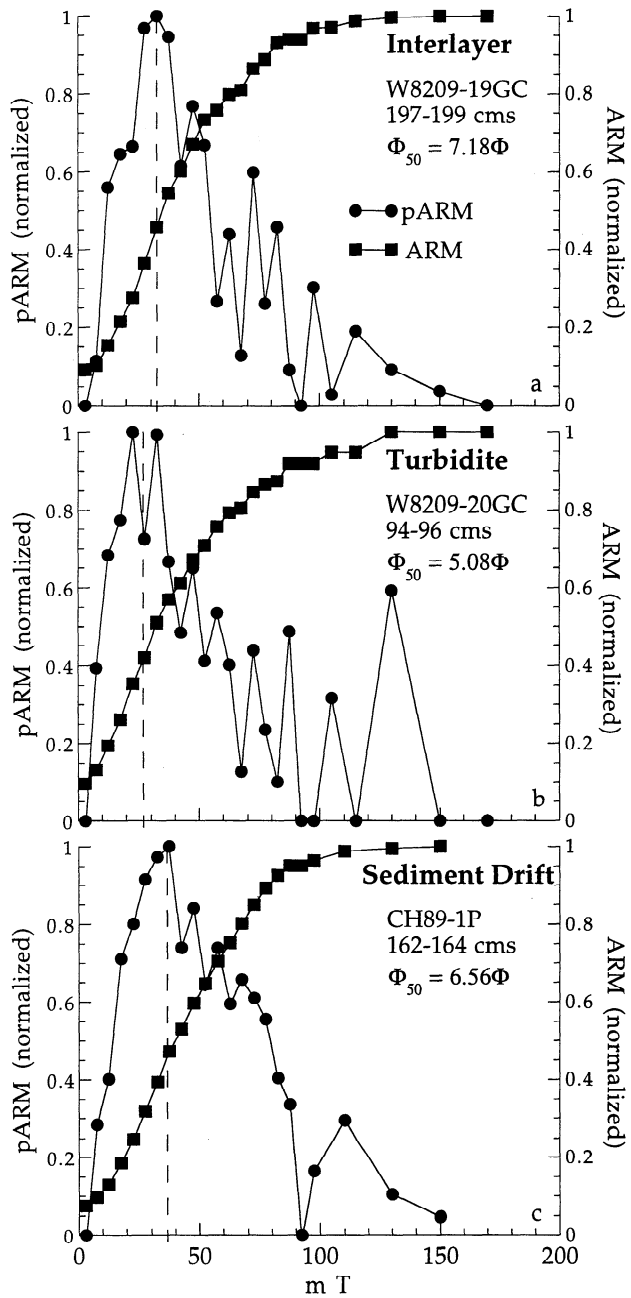

Figure 5. Partial anhysteric remanence magnetization (ARM). Magnetic grain size is indicated by the location of the peak of the partial ARM(pARM) curve, represented by the solid circles. The vertical dashed line represents the peak location in mT. Note that the peak for the (a) interlayer is at ~32 mT, approximately at the same location as the peak for the (b) turbidite at ~27 mT, and for the (c) drift at ~36 mT. This analysis does not show the significant difference in the magnetic grain size (all ~2 μm or 9Φ) exhibited among these three different environments' overall grain size analyses. The line with solid square symbols represents the normalized ARM. The line flattens out, implying magnetic grain saturation, at around 100 mT for all samples.

differences in magnetic grain size are unknown and are possibly very slight.

The trend in magnetic grain size does not follow that of the overall grain size trend (with the finest grains in the interlayers) and exhibits a much smaller grain size variation. This may result from a change in provenance (especially between the east and west coasts), from the differing density and settling capabilities of these grains (in this case, magnetite) versus those of clays, from the difference in the availability of certain grains for transport, from environmental energy, or even from the presence of in situ magnetotactic bacteria.

4. Interpretation

Both the grain size and magnetic fabric results cluster well by environment (Figure 4), with little overlap and few exceptions. Also notable on Figures 4a and 4b is the general relationship of the median grain size and P' with the probable velocity of the depositing current. As the interpreted current velocity increases from pelagic (effectively no current) to drift (generally <25 cms^{-1} but observed as fast as 70 cm/s^{-1} [*Bulfinch et al.*, 1982]) to turbidic (up to 100 cm/s^{-1} [*Bouma and Hollister*, 1973; *Nelson and Kulm*, 1973]), there is a general increase in median grain size (Figure 4a). In addition, the strength of the anisotropy (P') also increases as the interpreted current velocity of the depositing current increases (Figure 4b). This relationship of P' with current velocity implies that faster currents are able to align the sediment grains more effectively than slower currents and therefore impart a more pronounced magnetic fabric. Thus these trends represent the energy of the environments: interlayers represent low-energy, drifts are characteristic of intermediate-energy, and turbidites represent intermediate- to high-energy environments.

Potentially as significant as the trends themselves are the exceptions to these groupings; that is, those samples that do not fit within the defined limits of the environment from which they supposedly came. One of the exceptions, a sample from a depth of 102-104 cm in core CH89-1P, was deposited at the time of the Younger Dryas, a short period of pronounced cooling and changing oceanic circulation (10.3-9.05 radiocarbon ka [e.g. *Boyle and Keigwin*, 1987; *Haskell*, 1991; *Lehman and Keigwin*, 1992; *Keigwin and Jones*, 1994; *McCave et al.*, 1995a; B. Haskell, unpublished data, 1996]) within an overall warming trend. Therefore there may be a significant change in ocean circulation that occurs during this interval. Other possible explanations are that this interval may represent a layer rich in bacterial magnetite or may be one that has been diagenetically altered. *Schwartz et al.* [1997] noted that there is an iron maximum associated with a sulfur maximum at 110 cm depth in the CH89-1P core, which is thought to have resulted from a localized precipitation of iron sulfides in this area.

The complementary nature of grain size and magnetic fabric analyses for discrimination between depositional environments is illustrated by (1) the overlaps and (2) the exceptions. The depositional environments of samples that lie in the overlaps between the magnetic fabric trends can be evaluated using the grain size data, and vice versa. Either a misinterpretation of the depositional environment may occur or potentially important information about the environment may be lost when only one method is used. An example of this is the previously mentioned sample from the Younger Dryas period. This sample has a median grain size and sorting of a sediment drift but a strongly prolate magnetic fabric. The grain size information alone would indicate nothing extraordinary about this sample, whereas the magnetic fabric data alone may not adequately reflect the general depositional environment (i.e., the prolate shape may indicate

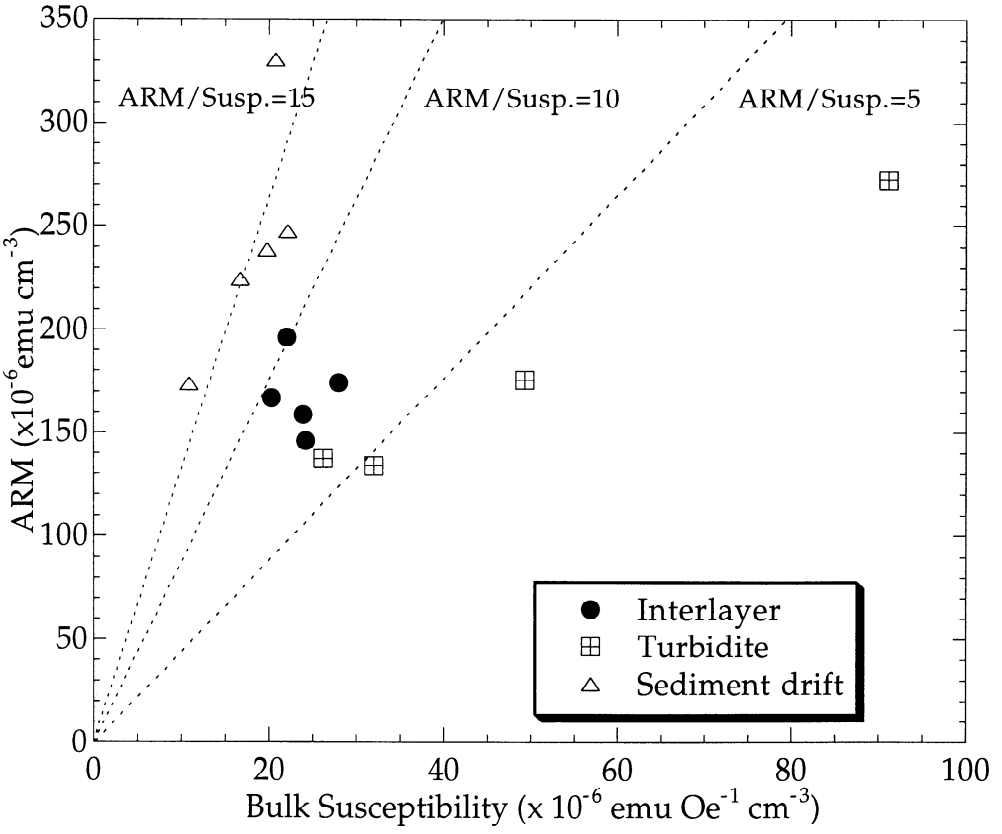

Figure 6. ARM versus bulk magnetic susceptibility. ARM is more sensitive to finer grains, while bulk susceptibility is more sensitive to relatively coarser grains. The high ARM to bulk susceptibility ratios that these samples exhibit are therefore indicative of fine grains. Notice how the samples plot in groups according to their depositional environment. The magnetic grain size of the sediment drifts is the finest while that of the turbidites is the coarsest. The sample with the highest bulk susceptibility on this plot is the turbidite sample where ferrimagnets dominated the magnetic susceptibility signal.

that secondary alteration of the sediment has occurred [*Schwartz et al.*, 1997; *Tauxe et al.*, 1990]). The combined data, however, indicate the special conditions for this sample.

To verify the usefulness of combined grain size and AMS analyses in defining depositional processes, two examples of previously identified "flow-in" (sediment that flows up into the piston core as a result of the suction generated by the piston) were analyzed. The samples, acquired from core W8709A-12PC located near the W8209 cores (Figure 1), were subjected to the same magnetic fabric and grain size analyses as the W8209 samples. The grain size results were not out of the ordinary; the flow-in samples fit well within the predicted interlayer trend (Figure 4a). However, the magnetic fabric data show that these samples are very peculiar (Figure 4b). The magnetic fabrics are strongly prolate, and the magnetic anisotropy directions show that the long axes of the grains in both flow-in samples were actually vertically oriented. While flow-in is not a natural depositional process, this test emphasizes the utility of the combined use of grain size and magnetic fabric analyses.

5. Alternative Origins of Magnetic Fabric

5.1. Compaction

As a sample gets buried, one would expect that the weight of the sediment column would compress and compact the sample. This may exhibit itself in our analyses by causing the magnetic fabric ellipsoid to become more oblate with depth as the minimum axis becomes shorter. Neither P' nor T show a regular variation with depth in any of the cores we investigated (including the BermudaRise core), indicating that this process does not significantly influence our magnetic fabric results.

5.2. Laboratory-induced AMS

Recent investigations by *Copons et al* [1997] indicate that sampling procedures may produce a magnetic fabric in soft, unlithified sediments. They found that the maximum susceptibility axis is parallel to the cutting surface, indicating that the grains had rotated during sample preparation. Our samples do not clearly exhibit this behavior.

5.3. Magnetotactic bacteria

Magnetite crystals produced by magnetotactic bacteria are far more abundant than the magnetites produced by other organisms [*Stolz et al.*, 1990, and references therein] and are ultra-fine single-domain grains [*Blakemore*, 1982; *Chang et al.*, 1987]. The biogenic production of these magnetites in the surface sediment could potentially influence magnetic measurements. The pARM experiments indicate that the magnetic grain sizes of our samples are ~2 μm, and the low temperature experiment did not indicate the presence of SP grains. *Peterson et al.* [1986] viewed the magnetic fraction of unconsolidated samples and noted that the coarser (μm-sized) grains were of a completely different type than the submicron

fraction, which were determined to be fossil magnetosomes of magnetotactic bacteria. This alleviates some concern of a major biologic influence on these samples. In addition, the low bulk magnetic susceptibilities of almost all of these samples indicate the domination of paramagnetic grains over ferrimagnetic grains. As well, the maximum axes of the AMS ellipsoids (not shown here) are better grouped than you would expect to see if the signal was dominated by bacterial grains. However, using different detection methods, the study by *Schwartz et al.* [1997] noted that bacterial magnetosomes are abundant in the top 95 cm of CH89-1P and are rare or absent below that depth. Only one of

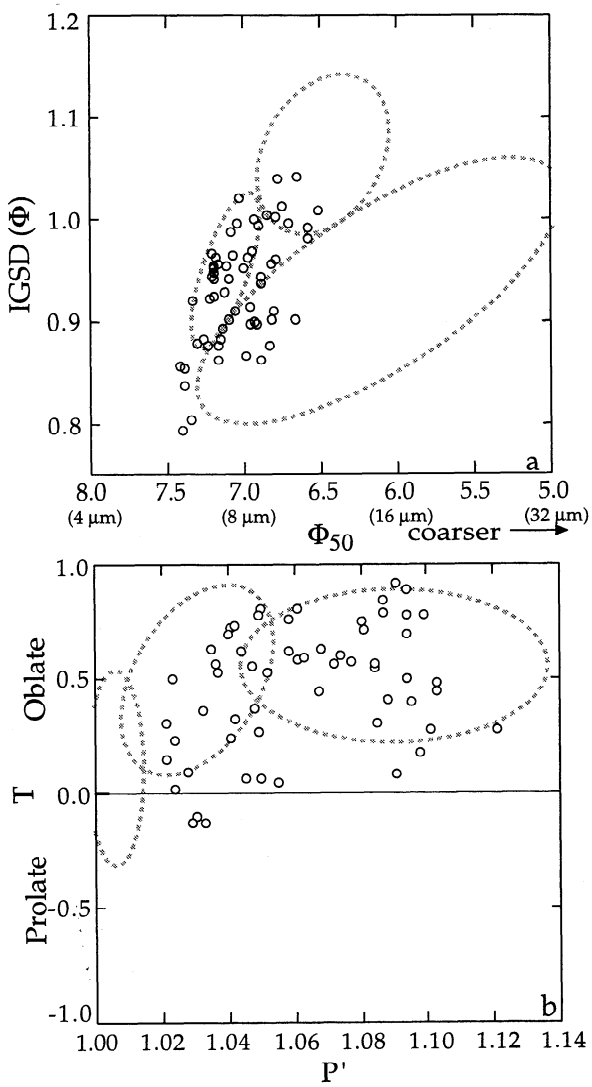

Figure 7. Grain size and magnetic fabric results from the Bermuda Rise sediment drift core: (a) median grain size (Φ_{50}) versus inclusive graphic standard deviation (IGSD) and (b) the strength of the anisotropy (P') versus the shape of the anisotropy (T). The dashed lines represent the depositional environment trends defined in Figure 4. Note that these sediment drift samples do not fall only within the sediment drift trend but generally have finer-grain sizes and the same or stronger magnetic fabrics than the sediment drift samples from the Blake Outer Ridge.

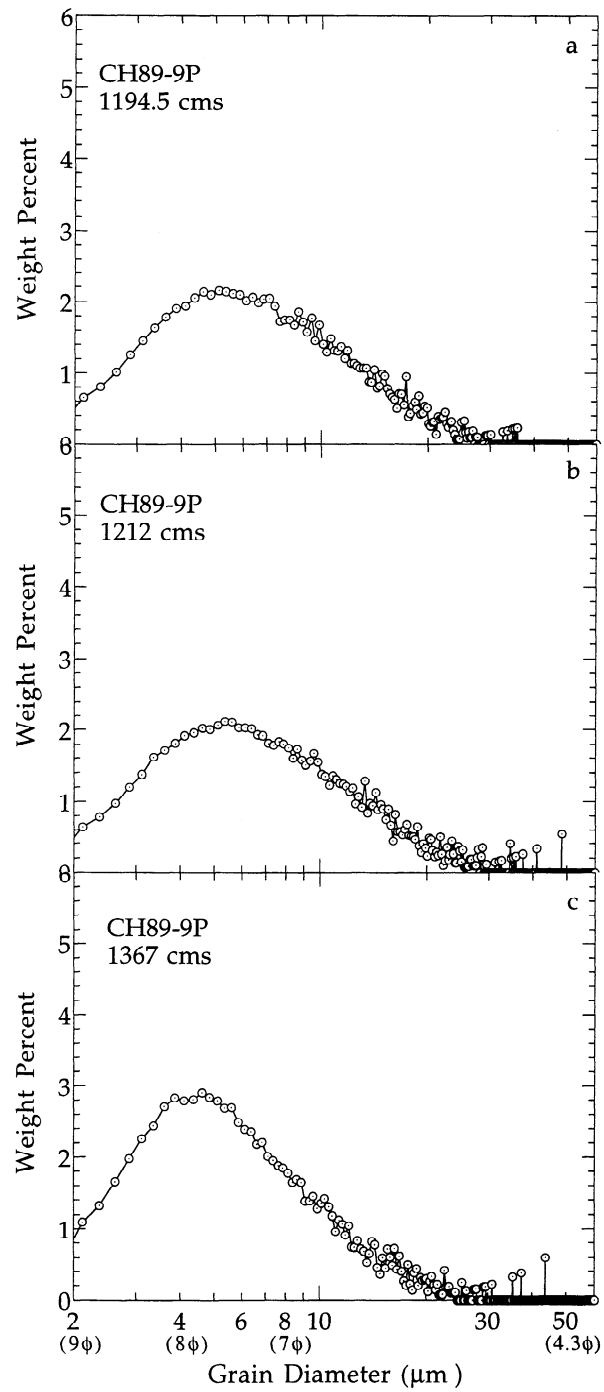

Figure 8. Grain size distributions of three Bermuda Rise cores. These three samples are examples of sediment with both median grain sizes and magnetic fabrics that lie within the turbidite field. While they may be interpreted as actually being turbidites (although it is not probable or noted at this location), their complete grain size distributions act as an additional discriminating factor in determining the depositional environment; these three samples resemble the sediment drift grain size distribution from Figure 3c, rather than the turbidite distribution (Figure 3b).

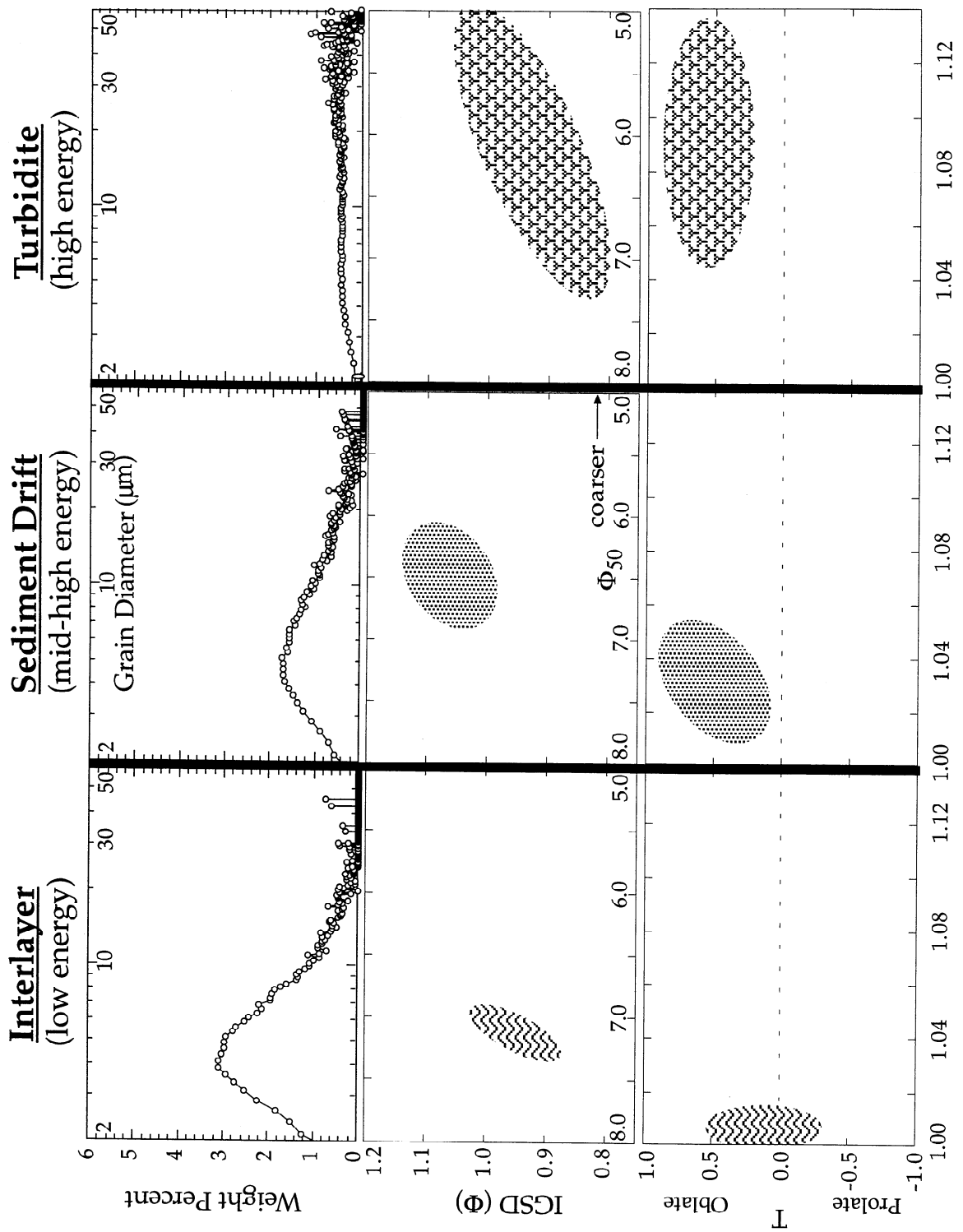

Figure 9. Summary of developed technique. Each column represents an environment of different depositional energy. The top row is a plot of a characteristic grain size distribution for each environment, while the two lower rows show the relationship of median grain size with the IGSD and P' with T, respectively. The shaded areas represent where samples deposited under the same depositional conditions would be expected to plot.

our samples analyzed for the magnetic grain size and type is in that upper interval, and this sample has the same properties as other samples. However, one of the findings of the study by *Schwartz et al.* [1997] is that while bacterial magnetosomes may be present and abundant in surficial sediment, the influence on many magnetic properties may be minimal for various reasons. Further studies of the effect that the presence of bacterial magnetite has on the intensity and shape of the AMS ellipsoid would be helpful in understanding how significant a factor bacterial magnetite is in our overall interpretation.

6. Application

With the grain size and magnetic fabric plots as our basis we interpret a second sediment drift core (Bermuda Rise core CH89-9P) according to the trends we have established. The Bermuda Rise samples have median grain sizes that vary between ~7.4 and 6.5Φ (5.9 and 10.8 μm) and IGSD's that extend from ~0.79 to 1.04Φ. In Figure 7a (Φ_{50} versus IGSD) the majority of the Bermuda Rise samples actually lie within the low-energy grain size trend as defined previously; the others are dispersed between both the intermediate- and high-energy areas. In contrast, none of the CH89-9P magnetic fabrics (Figure 7b) are contained within the low-energy magnetic fabric trend but range instead through the fields representative of intermediate- and high-energy processes. The magnetic fabric parameter P' ranges from 1.02 to 1.10, and ellipsoid shapes are almost entirely oblate. Low-temperature susceptibility experiments indicate that paramagnetic and ferrimagnetic grains both contribute to the AMS signal.

The samples from the Bermuda Rise are generally finer-grained than the Blake Outer Ridge samples. The relatively finer grains on the Bermuda Rise may result from a relatively lower current velocity or a smaller-sized sediment supplied to the core site. As none of these samples have magnetic fabrics that plot within the low-energy trend, we conclude that they have been exposed to current influence, often within the range of presumably intermediate- to high-energy velocities. Thus the finer grains are not the result of a drop in current velocity but instead are from differences in the nature of sediment being delivered to the site in relation to that at the Blake Outer Ridge. Even if the finer Bermuda Rise grains are more easily aligned than the coarser grains from the Blake Outer Ridge, the energy of the environment appears to be higher than the energy of the environment at the Blake Outer Ridge, a result that is not obvious from only the grain size data.

This interpretation is supported by noting the transport paths of the depositing currents. The western directed recirculating return flow of the Gulf Stream (Figure 2) is believed to be the depositing current for the Bermuda Rise. The current carries and redeposits the very fine grained portion of turbidites that have been resuspended from the Sohm Abyssal Plain and were originally derived from eastern Canadian sources (St. Lawrence [*Laine and Hollister,* 1981; *Keigwin et al.,* 1984]). Terrigenous sediment from northern sources is transported to the Blake Outer Ridge via the Western Boundary Undercurrent (WBUC), where the deflection of the WBUC by the Gulf Stream causes sediment deposition [*Heezen et al.,* 1966; *Haskell,* 1991; *Haskell and Johnson,* 1993]. Deposition of grains resuspended from an abyssal plain implies a finer-grain size than the deposition of grains derived directly from the continental margin. The original source of the grains may be similar for both locations.

Some of the samples in the Bermuda Rise core have both median grain sizes and magnetic fabrics that lie within the turbidite (high-energy) field. Although *Keigwin et al.* [1984] stated that there is no evidence of turbidites on Bermuda Rise, one might question whether these samples are indeed turbidites, rather than sediment deposited under generally high-energy drift conditions. However, one other discriminatory factor in this study is the complete grain size distribution (Figure 3). The complete grain size distributions of three of these samples (Figure 8), including those samples from 1212 and 1222 cm downcore with very strong magnetic fabrics (P' values of 1.12 and 1.10, respectively), are clearly more similar to sediment drift size distributions than the complete grain size distributions of turbidites (see Figure 3).

7. Conclusion

A distinction among depositional environments of terrigenous sediment is possible through the combined use of grain size and magnetic fabric analyses. These two methods are able to discriminate among sediment samples of turbidites, their pelagic or hemipelagic interlayers, and sediment drifts (Figure 9). In addition, there exists a relationship between the median grain size and intensity of anisotropy (P') with the interpreted current speed (both the median grain size and P' increase as the interpreted current speed increases). Commonly, the interlayer trends represent a very low energy environment, the drift samples represent an intermediate-energy environment, and the turbidites are characteristic of an intermediate- to high-energy environment.

We applied the grain size and magnetic fabric methods to a Bermuda Rise sediment drift core and interpreted the depositional conditions using our previously established trends. Whereas the fine terrigenous grains of the Blake Outer Ridge might be indicative of a lower-energy environment, the magnetic fabric indicates a pronounced current influence on these samples. High-energy sediment drift samples on the Blake Outer Ridge can be distinguished from turbidite sediments on the basis of their corresponding full grain size distributions (Figures 3 and 8). Overall, the magnetic fabric and grain size data suggest the presence of very high energy currents on Bermuda Rise.

Mean or median grain size is often used as the sole indicator of paleocurrent intensities [e.g., *Ledbetter and Johnson,* 1976; *Ledbetter,* 1984; *Haskell and Johnson,* 1993]. However, the use of grain size has been cited as an insufficient descriptor, as it may be influenced by changes in either source or supply [*Johnson et al.,* 1988; *McCave et al.,* 1995b]. Our study shows that the discrimination between very different depositional conditions is improved through the combined use of complete grain size distributions and magnetic fabric analyses. These techniques have the potential to contribute to the downcore interpretation of varying current strengths or depositional regimes, within a single geographic setting.

Acknowledgments. We thank the Oregon State University core laboratory for providing the samples from the *Wecoma* cores, T. Johnson for the samples from *Cape Hatteras* core 1P, and S. Lund for the *Cape Hatteras* core 9P samples. We also thank B. Haskell for providing his unpublished information on the CH89-1P core and E. Weber for his invaluable mechanical abilities. We greatly appreciate the input to this study provided by T. Moore and J. Parés. We thank J. King and two anonymous reviewers for their thorough and helpful reviews of this manuscript. L.J. acknowledges the financial support provided by a University of Michigan Regents' Fellowship.

References

Banerjee, S.K., J. King, and J. Marvin, A rapid method for magnetic granulometry with applications to environmental studies, *Geophys. Res. Lett., 8,* 333-336, 1981.

Blakemore, R.P., Magnetotactic bacteria, *Annu. Rev. Microbiol., 36,* 217-238, 1982.

Bouma, A.H., and C.D. Hollister, Part III: Deep ocean basin sedimentation, in *Turbidites and Deep-Water Sedimentation: Lecture Notes for a Short Course,* pp. 79-118, Pac. Sect., Soc. for Sediment. Geol., Los Angeles, Calif., 1973.

Boven, K.L., and D.K. Rea, Partitioning of eolian and hemipelagic sediment in eastern equatorial Pacific core TR163-31B and the late Quaternary paleoclimate of the northern Andes, *J. Sediment. Res., Sect. A,* in press, 1998.

Boyle, E.A., and L.D. Keigwin, North Atlantic thermohaline circulation during the past 20,000 years linked to high-latitude surface temperature, *Nature, 330,* 35-40, 1987.

Bulfinch, D.L., M.T. Ledbetter, and B.B. Ellwood, The high-velocity core of the Western Boundary Undercurrent at the base of the U.S. continental rise, *Science, 215,* 970-973, 1982.

Chang, S.R., J.F. Stolz, and J.L. Kirschvink, Biogenic magnetite as a primary remanence carrier in limestone, *Phys. Earth Planet. Inter., 46,* 289-303, 1987.

Clemens, S.C., and W.L. Prell, Late Pleistocene variability of Arabian Sea summer monsoon winds and continental aridity: Eolian records from the lithogenic component of deep-sea sediments, *Paleoceanography, 5,* 109-145, 1990.

Copons, R., J.M.Parés, J. Dinarès-Turell, and J. Bordonau, Sampling induced AMS in soft sediments: A case study in Holocene glaciolacustrine rhythmites from Lake Barrancs (Central Pyrenees, Spain), *Phys. Chem. Earth, 22,* 137-141, 1997.

Dunlop, D.J., Developments in rock magnetism, *Rep. Prog. Phys., 53,* 707-792, 1990.

Ellwood, B.B., and M.T. Ledbetter, Antarctic bottom water fluctuations in the Vema Channel: Effects of velocity changes on particle alignment and size, *Earth Planet. Sci. Lett., 35,* 189-198, 1977.

Ellwood, B.B., and M.T. Ledbetter, Paleocurrent indicators in deep sea sediment, *Science, 203,* 837-839, 1979.

Ellwood, B.B., M.T. Ledbetter, and D.A. Johnson, Sedimentary fabric: A tool to delineate a high-velocity zone within a deep western Indian Ocean bottom current, *Mar. Geol., 33,* 51-55, 1979.

Folk, R.L., *Petrology of Sedimentary Rocks,* 182 pp., Hemphill Publishing Company, Austin, Texas, 1974.

Freeman, R., The magnetization of some pelagic Tethyan limestones, Ph.D. dissertation, Eidg. Tech. Hochschule, Zurich, Switzerland, 1983.

Haskell, B.J., The influence of deep western North Atlantic circulation on late Quaternary sedimentation on the Blake Outer Ridge, Ph.D. dissertation, Duke Univ., Durham, N.C., 1991.

Haskell, B.J., and T.C. Johnson, Surface sediment response to deepwater circulation on the Blake Outer Ridge, western North Atlantic: Paleoceanographic implications, *Sediment.. Geol., 82,* 133-144, 1993.

Haskell, B.J., T.C. Johnson, and W.J. Showers, Fluctuations in deep western North Atlantic circulation on the Blake Outer Ridge during the last deglaciation, *Paleoceanography , 6,* 21-31, 1991.

Heezen, B.C., C.D. Hollister, and W.F. Ruddiman, Shaping the continental rise by deep geostrophic contour currents, *Science, 152,* 502-508, 1966.

Hovan, S.A., Late Cenozoic atmospheric circulation intensity and climatic history recorded by eolian deposition in the eastern equatorial Pacific Ocean: Leg 138 results, *Proc. Ocean Drill. Program Sci. Results, 138,* 615-625, 1995.

Jackson, M., W. Gruber, J. Marvin, and S.K. Banerjee, Partial anhysteretic remanence and its anisotropy: Applications and grainsize-dependence, *Geophys. Res. Lett., 15,* 440-443, 1988.

Jelinek, V., Characterization of the magnetic fabric of rocks, *Tectonophysics, 79,* 63-67, 1981.

Johnson, T.C., E.L. Lynch, W.J. Showers, and N.C. Palczuk, Pleistocene fluctuations in the Western Boundary Undercurrent on the Blake Outer Ridge, *Paleoceanography, 3,* 191-207, 1988.

Karlin, R., M. Lyle, and R. Zahn, Carbonate variations in the northeast Pacific during the late Quaternary, *Paleoc., 7,* 43-61, 1992.

Keigwin, L.D., and G.A. Jones, Glacial-Holocene stratigraphy, chronology, and paleoceanographic observations on some North Atlantic sediment drifts, *Deep Sea Res., Part A, 36,* 845-867, 1989.

Keigwin, L.D., and G.A. Jones, Western North Atlantic evidence for millennial-scale changes in ocean circulation and climate, *J. Geophys. Res., 99,* 12,397-12,410, 1994.

Keigwin, L.D., B.H. Corliss, E.R.M. Druffel, and E.P. Laine, High resolution isotope study of the latest deglaciation based on Bermuda Rise cores, *Quat. Res., 22,* 383-386, 1984.

King, J., S.K. Banerjee, J. Marvin, and O. Ozdemir, A comparison of different magnetic methods for determining the relative grain size of magnetite in natural materials: Some results from lake sediments, *Earth Planet. Sci. Lett., 59,* 404-419, 1982.

Laine, E.P., and C.D. Hollister, Geological effects of the Gulf Stream system on the northern Bermuda Rise, *Mar. Geol., 39,* 277-310, 1981.

Ledbetter, M.T., Bottom current speed in the Vema Channel recorded by particle size of sediment fine-fraction, *Mar. Geol., 58,* 137-149, 1984.

Ledbetter, M.T., and B.B. Ellwood, Spatial and temporal changes in bottom-water velocity and direction from analysis of particle size and alignment in deep-sea sediment, *Mar. Geol., 38,* 245-261, 1980.

Ledbetter, M.T., and D.A. Johnson, Increased transport of Antarctic Bottom Water in the Vema Channel during the last ice age, *Science, 194,* 837-839, 1976.

Lehman, S.J., and L.D. Keigwin, Sudden changes in North Atlantic circulation during the last deglaciation, *Nature, 356,* 757-762, 1992.

Lund, S.P., and L. Keigwin, Measurement of the degree of smoothing in sediment paleomagnetic secular variation records: An example from late Quaternary deep-sea sediments of the Bermuda Rise, western North Atlantic Ocean, *Earth Planet. Sci. Lett., 122,* 317-330, 1994.

McCave, I.N., B. Manighetti, and N.A.S. Beveridge, Circulation in the glacial North Atlantic inferred from grain-size measurements, *Nature, 374,* 149-151, 1995a.

McCave, I.N., B. Manighetti, and S.G. Robinson, Sortable silt and fine sediment size/composition slicing: Parameters for palaeocurrent speed and palaeoceanography, *Paleoceanography, 10,* 593-610, 1995b.

Nelson, C.H., and V. Kulm, Part II: Submarine fans and deep sea channels, in *Turbidites and Deep-Water Sedimentation: Lecture Notes for a Short Course,* pp. 39-78, Pac. Sect., Soc. for Sediment. Geol., Los Angeles, Calif., 1973.

Nye, J.F., *Physical Properties of Crystals,* 322 pp., Clarendon, Oxford, England, U.K., 1957.

Nye, J.F., *Physical Properties of Crystals,* 2nd ed.,, 329 pp., Clarendon, Oxford, England, U.K., 1985.

Petersen, N., T. von Dobeneck, and H. Vali, Fossil bacterial magnetite in deep-sea sediments from the South Atlantic Ocean, *Nature, 320,* 611-615, 1986.

Rea, D.K., and S.A. Hovan, Grain size distribution and depositional processes of the mineral component of abyssal sediments: Lessons from the North Pacific, *Paleoceanography, 10,* 251-258, 1995.

Rea, D.K., and T.R. Janecek, Mass accumulation rates of the non-authigenic inorganic crystalline (eolian) component of deep sea sediments from the western mid-Pacific mountains, Deep Sea Drilling Project Site 463, *Initial Rep. Deep Sea Drill. Proj., 62,* 653-659, 1981.

Rea, D.K., G.E. Ness, and G.R. Heath, Hemipelagic sedimentation in a region of crustal doming between the Mendocino and Pioneer fracture zones, *Mar. Geol., 62,*69-84, 1985.

Richter, C., and B.A. van der Pluijm, Separation of paramagnetic and ferrimagnetic susceptibilities using low temperature magnetic susceptibilities and comparison with high field methods, *Phys. Earth Planet. Int.er, 82,* 113-123, 1994.

Schwartz, M., S.P. Lund, D.E. Hammond, R. Schwartz, and K. Wong, Early sediment diagenesis on the Blake/Bahama Outer Ridge, North Atlantic Ocean, and it effects on sediment magnetism, *J. Geophys. Res., 102,* 7903-7914, 1997.

Shor, A.N., D.V. Kent, and R.D. Flood, Contourite or turbidite?: Magnetic fabric of fine-grained Quaternary sediments, Nova Scotia continental rise, in *Fine-Grained Sediments: Deep Water Processes and Facies,* edited by D.A.V. Stow and D.J.W. Piper, pp. 257-273, Blackwell Sci. Cambridge, Mass., 1984.

Stolz, J.F., D.R. Lovley, and S.E. Haggerty, Biogenic magnetite and the magnetization of sediments, *J. Geophys. Res., 95,* 4355-4361, 1990.

Stow, D.A.V., Distinguishing between fine-grained turbidites and contourites on the Nova Scotian deep water margin, *Sedimentology, 26,* 371-387, 1979.

Stow, D.A.V., and J.P.B. Lovell, Contourites: Their recognition in modern and ancient sediments, *Earth Sci. Rev., 14,* 251-291, 1979.

Tarling, D.H. and F. Hrouda, *The Magnetic Anisotropy of Rocks.,* 217 pp. Chapman and Hall, New York, 1993.

Tauxe, L., C. Constable, L. Stokking, and C. Badgley, Use of anisotropy to determine the origin of characteristic remanence in the Siwalik Red Beds of Northern Pakistan, *J. Geophys. Res., 95,* 4391-4404, 1990.

L.H. Joseph, D.K. Rea, and B.A. van der Pluijm, Department of Geological Sciences, University of Michigan, Ann Arbor, MI 48109-1063.(email: ljoseph@umich.edu)

(Received September 11, 1997;
revised June 4, 1998;
accepted June 4, 1998.)